Neutron-proton equilibration in 35 MeV/u collisions of ^{64,70}Zn + ^{64,70}Zn and ^{64}Zn,^{64}Ni + ^{64}Zn,^{64}Ni quantified using triplicate probes

L. W. May,[1,2,*] A. Wakhle,[2] A. B. McIntosh,[2] Z. Kohley,[1,2] S. Behling,[2,3] A. Bonasera,[2] G. Bonasera,[2,3] P. Cammarata,[1,2] K. Hagel,[2] L. Heilborn,[1,2] A. Jedele,[1,2] A. Raphelt,[1,2] A. Rodriguez Manso,[2] G. Souliotis,[2,4] R. Tripathi,[2] M. D. Youngs,[2] A. Zarrella,[1,2] and S. J. Yennello[1,2]

[1]*Chemistry Department, Texas A&M University, College Station, Texas, USA*

[2]*Cyclotron Institute, Texas A&M University, College Station, Texas, USA*

[3]*Physics Department, Texas A&M University, College Station, Texas, USA*

[4]*Laboratory of Physical Chemistry, Department of Chemistry, National and Kapodistrian University of Athens, Athens 15771, Greece*

(Received 16 May 2018; revised manuscript received 16 August 2018; published 3 October 2018)

Previous work has quantified the degree of neutron-proton equilibration in heavy-ion nuclear collisions by observing the convergence of isospin observables (such as the isoscaling parameter α) to an expected value based on similar symmetric reaction systems. We present a new signature of equilibration: the convergence of the isospin asymmetry (as quantified by three isoscaling metrics) of two mirror asymmetric reaction systems toward each other rather than a predefined point. For the reactions of 35 MeV/u ^{64,70}Zn + ^{64,70}Zn and ^{64}Zn, ^{64}Ni + ^{64}Zn, ^{64}Ni the neutron-proton equilibration was found to be approximately 80%, and this result is compared directly to previous work.

DOI: 10.1103/PhysRevC.98.044602

I. INTRODUCTION

The nuclear equation of state (EOS) represents the relationship between thermodynamic variables that describe the nature of nuclei and nuclear matter. An improved understanding of the EOS and the form of the asymmetry energy provides information relating to fundamental nucleon-nucleon interactions, nuclear structure, nuclear reactions, and astrophysical processes such as the core collapse of supernovae, dynamics of neutron star mergers, and properties of neutron star crusts [1–7]. Particular effort has been made to improve experimental constraints on the density dependence of the asymmetry energy, the term with the largest uncertainty in the EOS.

While the asymmetry energy of nuclear matter is relatively well understood in the ground state [6], heavy-ion collisions provide the ability to probe the EOS away from ground-state density and temperature. Numerous experiments have been conducted in order to place constraints on the density dependence of the asymmetry energy through a variety of experimental observables such as free neutron-proton ratios [6,8,9], isobaric yield ratios [10–13], isoscaling [12,14–25], isospin diffusion [2,21,26–30], collective flow [31–37], and neck dynamics and emission [38–44].

Early neutron-proton (N-Z) equilibration work, also referred to as isospin equilibration in the literature, used isotopic ratios to demonstrate the beam energy dependence of equilibration in the Fermi energy regime [45–48]. Ideally we would like to measure the composition of the quasiprojectile (QP, the primary, excited, projectile-like fragment immediately following the collision), quasitarget (QT), and any remaining neck-like structure immediately after separation. This would give an exact measure of the amount of equilibration in a nuclear reaction. Thus the isospin asymmetry of the QP ($\Delta_{\rm QP} = \frac{N_{\rm QP}-Z_{\rm QP}}{A_{\rm QP}}$) could be compared to the isospin asymmetry of the projectile and target in order to calculate the amount of equilibration [10]. Measurement of the composition of the QP accurately would require an 8π detector system. Fragmentation of the QP due to excitation energy, as well as evolution of the system due to pre-equilibrium emission, further complicates this comparison and will not yield a complete description of the equilibration of the system. In reality, observables that were linearly dependent [10,29] on the isospin composition of a source were used as surrogates for the actual $\Delta_{\rm QP}$. Several observables have been suggested that fit this criterion including free n/p ratios [6,9], isobaric yield ratios [11,13,29], charged pion ratios [9], and the isoscaling parameter α [10,17,18,21]. The degree of equilibration can be quantified by determining isospin asymmetry of the hot source after the reaction, and comparing it to the initial state.

Using these surrogates we can construct the isospin transport ratio [Eq. (1), henceforth referred to as R_i), a means of quantifying the degree of equilibration in a reaction. This concept was originally formulated by Rami *et al.* [49] and has been used in a multitude of studies to measure equilibration in nuclear systems [2,6,10,21,29,38,49–55]. Equation (1) quantifies the position of an observable for a specific source (x_i) relative to the same observable for a different source ($x_{i'}$). A neutron-rich source ($x_{\rm NR}$) will give a value of $R_{\rm NR} = 1$ and a neutron-poor source ($x_{\rm NP}$) will give $R_{\rm NP} = -1$, so that any source that is mixed between these will yield an R_i value

*lmay@comp.tamu.edu

between −1 and 1.

$$R_i = \frac{2x_i - x_{\rm NR} - x_{\rm NP}}{x_{\rm NR} - x_{\rm NP}}. \quad (1)$$

Rami *et al.* [49] showed that more central collisions lead to more equilibration, i.e., a greater degree of equilibration was observed for smaller impact parameters. Central reactions provide a greater overlap between projectile and target, and therefore more damping and longer contact times. These longer contact times between projectile and target allow more equilibration to take place [56–58]. Thus signatures of equilibration are expected to be more pronounced in strongly damped or more central collisions [59].

Since the R_i was introduced, many studies have continued to probe *N-Z* equilibration in reactions around the Fermi energy. Experimental [2,6,10,19,21,28,29,50,60–64] as well as theoretical [26,27,53,65,66] efforts have attempted to place stricter constraints on the asymmetry energy. A recent review [67] concluded that experimental, theoretical, and observational analyses constrain the symmetry parameters S_0 and L to 29.0–32.7 MeV and 40.5–61.9 MeV, respectively. This review did not address higher-order cubic and quartic terms. With knowledge of only the first two terms in the Taylor series expansion, any extrapolation away from saturation densities (to subsaturation and supersaturation) is prone to large uncertainties due to these higher-order terms.

In the present work we will use isoscaling, isobaric yield ratios, and reconstructed QP asymmetry from the NIMROD array to measure the amount of *N-Z* equilibration that takes place between the QP and QT. This will be directly compared to previously reported values of fractional equilibration.

II. EXPERIMENTAL

The NIMROD 4π array at Texas A&M University [68] was used to study the reactions ^{64,70}Zn + ^{64,70}Zn and ^{64}Zn, ^{64}Ni + ^{64}Zn, ^{64}Ni at 35 MeV/u. Details of the setup have been described in Refs. [31,32,68,69] and will not be discussed here. The array achieved isotopic identification of fragments up to $Z = 17$ and elemental identification up to $Z = 30$. This exceptional sensitivity allows the kinematic reconstruction of the hot QP immediately after interaction and reseparation. Such reconstruction dramatically improves the quality of source selection as well as isoscaling fits [23,70].

To ensure a well-defined QP source, a series of constraints were placed on the reconstruction. These constraints allow selection of thermally equilibrated QP sources [71–74]. The first constraint is a cut on the velocity in the direction of the beam of individual fragments which excludes fragments that do not originate from the QP (fast pre-equilibrium emission as well as particles from QT-like sources). By comparing individual fragment velocities, v_z, to that of the largest fragment in the event, $v_{z,\rm res}$, particles that have velocities consistent with pre-equilibrium emission or midrapidity sources are excluded. Numerically, this cut only includes fragments whose velocities fall into the following ranges: $\frac{v_z}{v_{z,\rm res}} = 1 \pm 0.65$ for $Z = 1$, $\frac{v_z}{v_{z,\rm res}} = 1 \pm 0.60$ for $Z = 2$, and $\frac{v_z}{v_{z,\rm res}} = 1 \pm 0.45$ for $Z \geqslant 3$.

A wide mass range was considered to reconstruct the QP in order to cover all possible reaction channels leading to fragmentation. The reconstructed QPs were selected to have a total proton number (Sum$Z$) fulfilling the requirement $15 \leqslant {\rm Sum}Z \leqslant 35$ and total nucleon number (Sum$A$) fulfilling the requirement $48 \leqslant {\rm Sum}A \leqslant 76$. Narrower cuts on reconstructed Sum$Z$ had no appreciable effect on the values in the analysis, only on the level of statistics. Utilizing such a large mass and charge range also provides a large variability in possible QP asymmetries for study.

A final cut is applied to constrain the shape of the QP. Shape equilibration is a much slower process than either thermal or *N-Z* equilibration [75] and therefore a spherical QP should be well equilibrated. Spherical QPs are selected by examining the relationship between the total particle momentum in the beam direction, p_z, relative to the transverse momentum, p_t, such that the sphericity of the event is $S_{\rm event} = \frac{\sum p_z^2}{2 \cdot \sum p_t^2}$ where the sum is over all charged particles in the associate with the QP in the event.

Previous work has shown both the benefits of including the free neutrons in source reconstruction [23,72,76], as well as the possible concerns and uncertainty [76,77]. Free neutrons were used in this analysis only in the reconstruction of the QP and in the determination of the reconstructed total nucleon number.

III. ANALYSIS AND CONCLUSIONS

Isotopically identified fragments from reconstructed QPs were used to calculate the ratio of yields of each of the seven reactions to the yields of the most neutron-poor reaction: ^{64}Zn + ^{64}Zn. Two sets of reactions were analyzed. The first reaction set, ^{64,70}Zn + ^{64,70}Zn, compares the cross reactions formed by two different isotopes of zinc, producing a set of reactions that displays an isospin asymmetry difference between projectile and target, with no Coulomb difference between projectile and target. A set of reactions with these properties has also been studied in Ref. [21]. In the present work, we additionally study the ^{64}Zn, ^{64}Ni + ^{64}Zn, ^{64}Ni reaction set. The ^{64,70}Zn + ^{64,70}Zn reaction set holds Z constant but varies asymmetry by varying reactant mass A. The ^{64}Zn, ^{64}Ni + ^{64}Zn, ^{64}Ni reaction set holds A constant but varies the asymmetry by changing reactant proton number Z. This choice of reactions was made to isolate the individual effects of these changes on the overall dynamics of isospin transport.

The ratio of the yields of a neutron-rich source Y_2 to a neutron-poor source Y_1 are compared for a range of isotopically identified fragments. The yield ratio, shown in Eq. (2), is parametrized by the exponential form shown in Eq. (3), where C is a scaling constant and α and β are the isoscaling parameters for neutrons and protons, respectively [21].

$$R_{21}(N, Z) = \frac{Y_2(N, Z)}{Y_1(N, Z)}, \quad (2)$$

$$R_{21}(N, Z) = C \exp(\alpha N + \beta Z). \quad (3)$$

The isoscaling parameter α is assumed to be linearly dependent on the source asymmetry in isospin transport studies [10,17,18,21,29]. The parameters α and β are linearly related

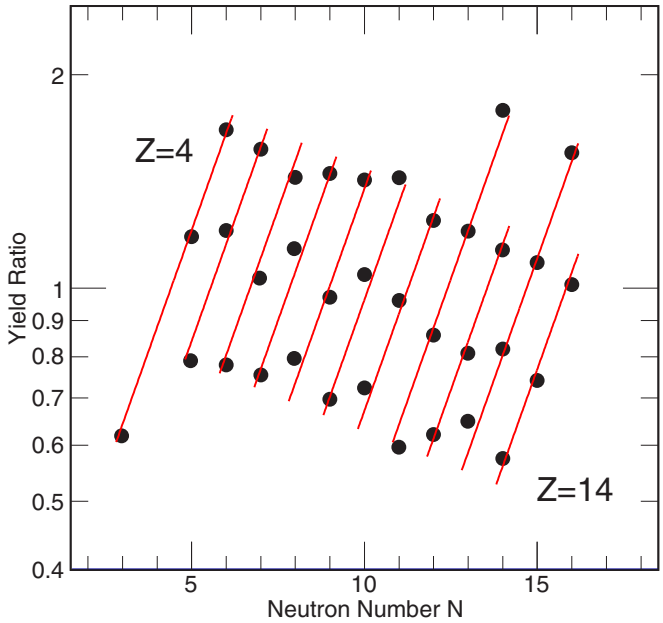

FIG. 1. An example isoscaling plot using an expanded Z range in fragments. The plot shows the isoscaling of abundant isotopes from $Z = 4$–14 for the ^{64}Ni + ^{64}Ni system relative to the ^{64}Zn + ^{64}Zn system. The red fit lines correspond to the resulting global fit according to Eq. (3).

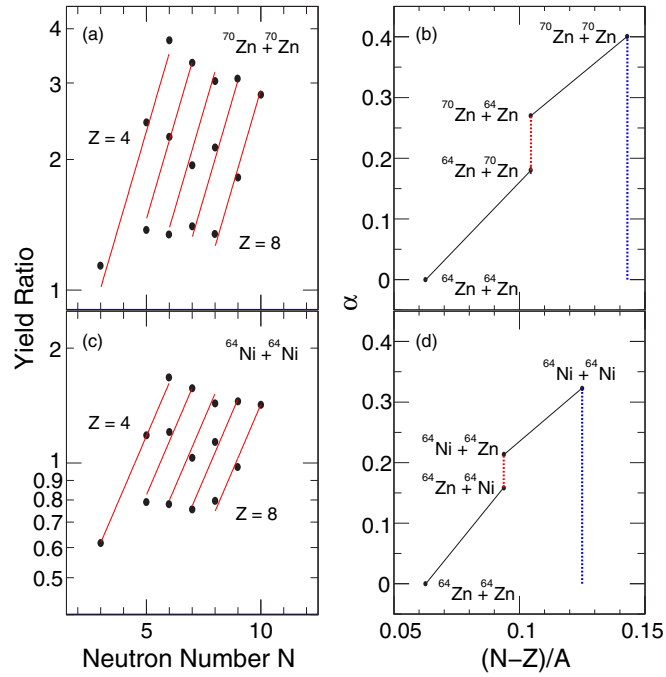

FIG. 2. Isoscaling plots for the Zn (^{64,70}Zn + ^{64,70}Zn) and $A = 64$ (^{64}Zn, ^{64}Ni + ^{64}Zn, ^{64}Ni) reactions. Panel (a) shows the yield ratios as a function of neutron number N for the three most abundant isotopes of $Z = 4$–8 for the ^{70}Zn + ^{70}Zn system, and panel (c) corresponds to the three most abundant isotopes of $Z = 4$–8 for the ^{64}Ni + ^{64}Ni system. Panel (b) is a plot of α (see text for details) as a function of composite system isospin asymmetry for the Zn set of reactions, and panel (d) corresponds to the $A = 64$ set of reactions.

to the chemical potentials, which depend on the local density and asymmetry and influence the migration of neutrons.

An example isoscaling plot is shown in Fig. 1. The yield ratio from Eq. (2) is plotted as a function of neutron number for isotopes of all elements from beryllium to silicon ($Z = 4$–14). Note that yields from the ^{64}Ni + ^{64}Ni reaction were divided by the yields from the ^{64}Zn + ^{64}Zn reaction. Error bars representing statistical error are included here and for all subsequent figures and are typically smaller than the data points. For any given element, the yield ratio increases monotonically with the neutron number. The solid red curves represent a single exponential fit of the data in both Z and N space simultaneously using the parametrization in Eq. (3). Thus the curves have the same exponential slope and are equally spaced. The exponential fit describes the data well, and deviations from the fit line follow no clear systematic trend. This indicates that reaction mechanisms such as isospin density gradients driving equilibration, observed in other experimental data [1,26], are observed here as well. Also, isoscaling is observed for all fragment sizes presented, indicating that these fragments originate from sources that have achieved the same degree of equilibration.

The left panels of Fig. 2 show plots of the yield ratio as a function of neutron number for isotopes of all elements from beryllium to oxygen ($Z = 4$–8). Ratios from the most neutron-rich reactions, with respect to the most neutron-poor system, in each set are shown: Fig. 2(a) for ^{70}Zn + ^{70}Zn and Fig. 2(c) for ^{64}Ni + ^{64}Ni. The limited range in Z was used to allow a direct comparison with Ref. [21]. Again, the red curves represent the result of one single exponential fit to all the data points using the parametrization of Eq. (3). The yield ratios increase monotonically with the neutron number, and the resulting curves have the same exponential slope and are equally spaced, demonstrating a clear scaling between isotopes that is consistent with previous measurements for similar systems [23].

The isoscaling parameter α is used as a surrogate for the isospin asymmetry of the quasiprojectile, and as a way to assess the degree of N-Z equilibration. In fully N-Z equilibrated reactions, the QP and QT should exhibit identical isospin asymmetries. Mirror reactions, such as ^{64}Ni + ^{64}Zn and ^{64}Zn + ^{64}Ni, are identical if the target and projectile are swapped. Thus the QP of one system will be identical to the QT of the other system. If the cross systems have reached full N-Z equilibration, their isoscaling parameters α should be identical.

Figures 2(b) and 2(d) show the isoscaling parameter α as a function of the composite system asymmetry $\frac{(N-Z)}{A}$. Solid black lines connect systems with the same projectile. The solid red and solid blue lines represent the separation between two cross systems, and two symmetric systems, respectively. The isoscaling parameter α of the cross reactions differs from that of the symmetric reactions. This can be interpreted as a degree of mixing, but not complete mixing, between the projectile and target. If the projectile and target mix completely, then there would be no difference between two cross reactions, and their α values would be the same.

This metric of isospin transport has been the basis of measurements of equilibration in previous works. However, the cross reactions are not centered about the average α values of the symmetric systems in either set of reactions. This is evident in Ref. [21] as well. The R_i used in that work assumes that a fully N-Z equilibrated cross system will be halfway between that of the two symmetric systems from the same reaction set. This assumption is limiting because the equilibrium value of isospin, or the equilibrium value of α, need not necessarily be half way between the values for the symmetric systems. It could be that for a large amount of mixing the reaction mechanism changes such that significant mass is lost in the early phase of the reaction, and the isospin of the lost mass is neutron rich thus affecting the equilibrium value of the isospin of the remaining, relatively neutron-poor system. This limitation led us to develop a new measure for equilibration that is not dependent on reaching a predefined endpoint. This measure of the equilibration in a reaction quantifies the convergence of cross systems toward each other, relative to the difference between the symmetric systems.

Equation (4) (based on Ref. [62]) is used to compare the linearly dependent isospin observables of all reactions in a reaction set. The variables x_{xS1} and x_{xS2} are the first and second cross systems ^{70}Zn + ^{64}Zn and ^{64}Zn + ^{70}Zn, respectively. By comparing the separation between cross systems (x_{xS1}-x_{xS2}) to the separation between symmetric systems ($x_{\rm NR}$-$x_{\rm NP}$), a value of fractional equilibration $\Gamma_{\rm eq}$ can be extracted. A value of 0 indicates cross systems that are identical to the symmetric reaction systems, while a $\Gamma_{\rm eq}$ of 1 indicates that the two cross systems are identical to each other. The advantage of this method is that any differential loss outside of the QP-QT pair, through pre-equilibrium particle emission or neck formation, does not affect the calculation of how much equilibration has taken place.

$$\Gamma_{\rm eq} = \frac{(x_{\rm NR} - x_{\rm NP}) - (x_{xS1} - x_{xS2})}{(x_{\rm NR} - x_{\rm NP})}. \tag{4}$$

This method of calculating the fractional equilibration between QP and QT can be extended to study equilibration as a function of the impact parameter b. Calculations using the ASY-SOFT constrained molecular dynamics (CoMD) code [78,79] were used to identify an observable related to the impact parameter. The reconstructed QP velocity ($v_{z,\rm QP}$) parallel to the beam showed the strongest correlation with impact parameter, compared to excitation energy and QP deflection angle. The top panels of Fig. 3 show the reconstructed QP velocity in the laboratory frame as a function of the event impact parameter b. We see a monotonic correlation between $v_{z,\rm QP}$ and b for $b > 2$ fm. A simple function correlating the variables $v_{z,\rm QP}$ and b was extracted from this. The data were partitioned into ten bins in $v_{z,\rm QP}$ (Fig. 3 bottom panel) such that there was approximately equal data in each bin. While the bins overlap, the peaks are separated well enough to observe a general trend of smaller $v_{z,\rm QP}$ values corresponding to smaller impact parameters, or violent collisions. This allows the analysis of N-Z equilibration as a function of the violence of the collision using $v_{z,\rm QP}$ bins as surrogates for impact parameter bins.

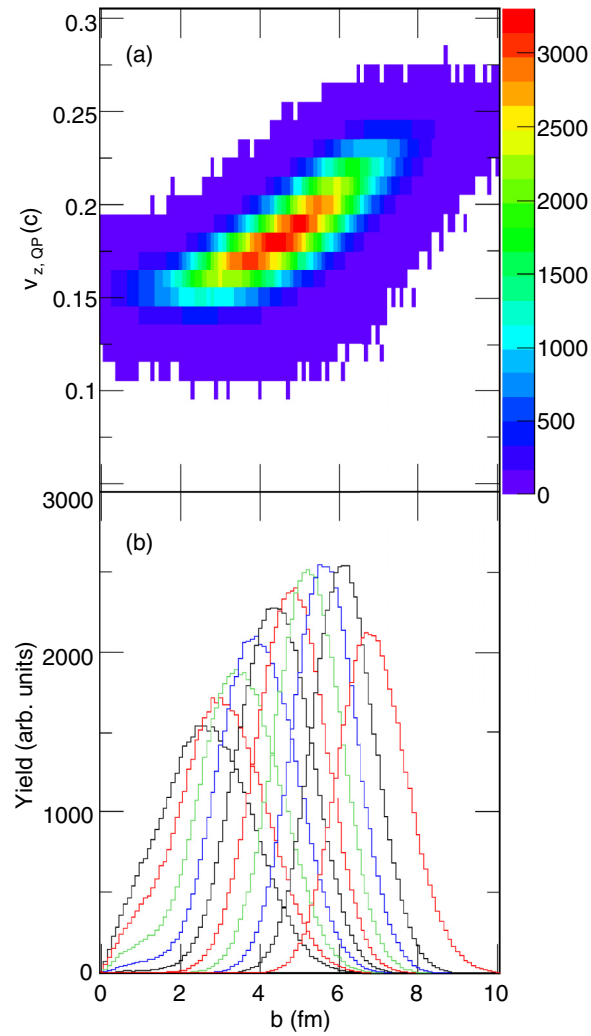

FIG. 3. (a) Reconstructed QP velocity in the parallel beam direction (in units of c) in the laboratory frame as a function of the event impact parameter b (in fm) from ASY-SOFT CoMD simulation of the ^{64}Ni + ^{64}Ni system. (b) Resulting distribution of b in each of the nine QP v_z bins.

This surrogate for impact parameter, and violence of collision, was used along with three separate metrics to quantify N-Z equilibration: 1) The isoscaling parameter α as discussed above; 2) the isobaric yield ratio of tritons to helium-3 $Y(^3\mathrm{H})/Y(^3\mathrm{He})$; and 3) the reconstructed QP asymmetry $\Delta_{\rm QP}$. The evolution of these isospin-dependent metrics, as a function of violence of collision, is studied using R_i [Eq. (1)].

A. Isoscaling parameter α

We calculate fractional equilibration $\Gamma_{\rm eq}$ by substituting the isoscaling parameter α for x in Eq. (4) for each bin in $v_{z,\rm QP}$. In this way, we can examine $\Gamma_{\rm eq}$ as a function of collision violence. In Fig. 4, R_i is plotted as a function of $v_{z,\rm QP}$ for the $A = 64$ reactions relative to the neutron-poor ^{64}Zn + ^{64}Zn reaction. We recall that by definition R_i is 1 or -1 for the symmetric reactions, and that R_i values are expected to converge for the cross reactions relative to the symmetric

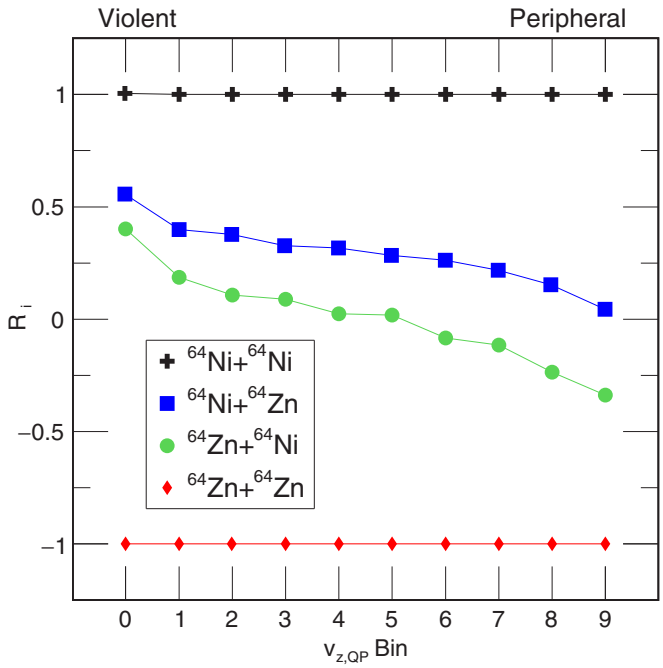

FIG. 4. Isospin transport ratio (R_i) value [Eq. (1)] for the isoscaling α parameter as a function of $v_{z,QP}$ bin number from experimental data. Lower $v_{z,QP}$ bin number on average means a more central collision. This shows the results from the $A = 64$ set of reactions: ^{64}Zn + ^{64}Zn, ^{64}Zn + ^{64}Ni, ^{64}Ni + ^{64}Zn, and ^{64}Ni + ^{64}Ni.

reactions. The R_i for cross reactions in Fig. 4 converge toward each other as the reactions become more violent ($v_{z,QP}$ bin = 0), indicating that the QP and QT are becoming more similar in isospin as the violence of the collision increases. The R_i values show substantial equilibration for even the most peripheral collisions analyzed ($v_{z,QP}$ bin = 9).

The equilibration observed at large $v_{z,QP}$ may also be partly due to overlapping $v_{z,QP}$ bins. Bin 9 of $v_{z,QP}$ is peaked at b = 7 fm, whereas touching spheres is estimated at $b = 10$ fm for these reactions. Although $v_{z,QP}$ of 9 corresponds to the most peripheral reactions in these data, more peripheral collisions are physically possible, where a smaller Γ_{eq} is expected.

Two different isotopic ranges were used to extract Γ_{eq}: a shortened range from $Z = 4$–8 using only the three most prominent isotopes to compare to Ref. [21], and an expanded range using all isotopically identified fragments ($Z = 4$–14) from the NIMROD array. The ^{64}Zn, ^{64}Ni + ^{64}Zn, ^{64}Ni reactions yield a Γ_{eq} of 0.83 ± 0.05 for the shortened Z range, and 0.85 ± 0.07 for the full Z range. For the ^{64,70}Zn + ^{64,70}Zn reactions we calculate a Γ_{eq} of 0.78 ± 0.05 for the shortened Z range, and 0.76 ± 0.07 for the full Z range. These values are reported in Table I. The differences in Γ_{eq} experienced by the charge symmetric systems (^{64,70}Zn + ^{64,70}Zn) vs the charge asymmetric systems (^{64}Zn, ^{64}Ni + ^{64}Zn, ^{64}Ni) agree within experimental uncertainty. The effect of the Coulomb asymmetry does not seem to be at play at this level of sensitivity. The uncertainties quoted here are dominated by the uncertainty in the yields of each isotope due to contamination from neighboring isotopes.

In Ref. [21] the Γ_{eq} in 50 MeV/u ^{124,112}Sn + ^{124,112}Sn reactions was reported as ∼0.5. Applying Eq. (4) to the α values of that work we calculate a Γ_{eq} of 0.54 ± 0.02. This is also reported in Table I along with the Γ_{eq} values for reactions studied in this work (discussed subsequently).

B. Isobaric yield ratio

The isobaric yield ratio (IYR) employs a single source as the isospin-dependent metric, and in previous work has exhibited linear dependence on the isospin asymmetry of the source [73,76]. The ratio of the yields of two isobars are used; the yield of the neutron-rich isotope ($Y_{A,NR}$) is normalized to the yield of the neutron-poor isotope ($Y_{A,NP}$):

$$\text{Isobaric yield ratio} = \frac{Y_{A,NR}}{Y_{A,NP}}. \quad (5)$$

The $A = 3$ isobars, tritium and helium-3, are used to examine how the collision violence impacts the extent of N-Z equilibration. The $A = 7$ isobaric yield ratios show the same trend as the $A = 3$. The raw isobaric yield ratio $Y(^3H)/Y(^3He)$ is plotted as a function of $v_{z,QP}$ in Fig. 5 top (panel a). The isobaric yield ratio shows an overall increase with increasing collision violence (decreasing $v_{z,QP}$). To quantify the extent of N-Z equilibration, we plot R_i as a function of collision violence in Fig. 5(b). The R_i value is obtained by substituting the isobaric yield ratio in Eq. (1). The convergence of the cross reactions with increasing collision violence is more apparent after this transformation. Figure 5(b) appears to show a smaller degree of equilibration for peripheral collisions relative to Fig. 4, and comparable equilibration for violent collisions. Isoscaling is known to be sensitive to secondary decay [73]. It may be that the $A = 3$ isobaric yield ratio probe is less sensitive to secondary decay, since copious amounts

TABLE I. Fractional equilibration Γ_{eq} calculated from experimental data based on the isoscaling metrics used in this work.

Equilibration metric	35 MeV/u ^{64,70}Zn + ^{64,70}Zn	35 MeV/u ^{64}Zn, ^{64}Ni + ^{64}Zn, ^{64}Ni	50 MeV/u ^{124,112}Sn + ^{124,112}Sn [21]
Isoscaling α ($Z = 4$–8)	0.78 ± 0.05	0.83 ± 0.05	0.54 ± 0.02
Isoscaling α ($Z = 4$–14)	0.76 ± 0.07	0.85 ± 0.07	
$Y(^3H)/Y(^3He)$	0.72 ± 0.04	0.77 ± 0.04	
Δ_{QP}	0.96 ± 0.05	0.85 ± 0.05	

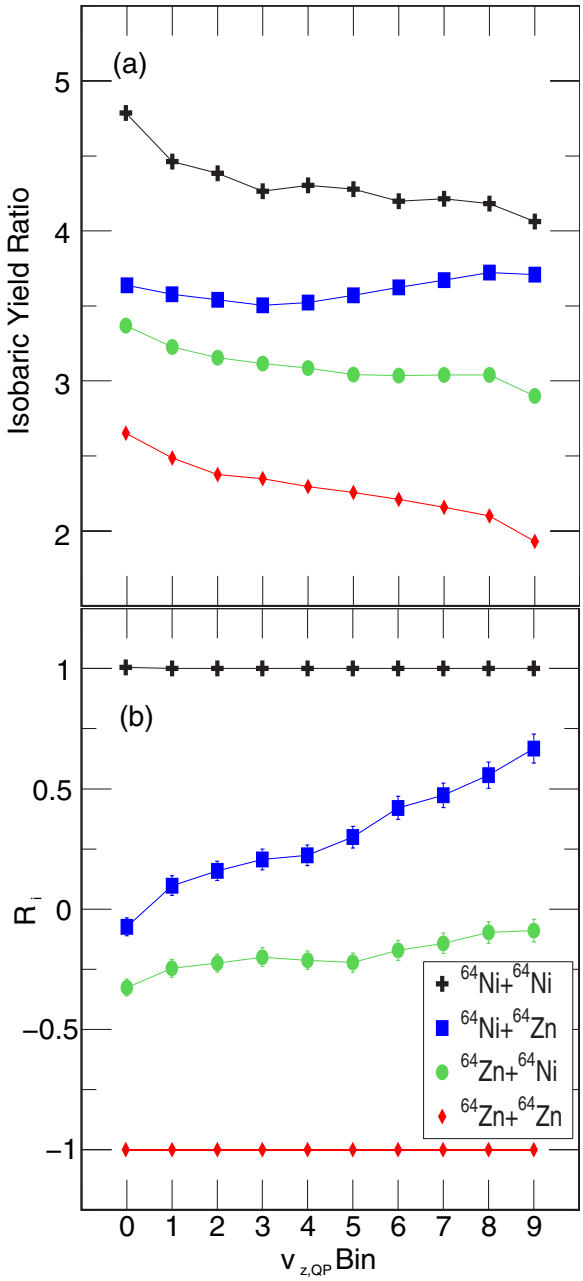

FIG. 5. (a) Isobaric yield ratio and (b) isospin transport ratio R_i for $A = 3$ isobar as functions of $v_{z,QP}$ bin for the $A = 64$ set of reaction systems: ^{64}Ni + ^{64}Ni, ^{64}Ni + ^{64}Zn, ^{64}Zn + ^{64}Ni, and ^{64}Zn + ^{64}Zn.

at $A = 3$ particles are produced in the initial stages of the reaction. The stronger dependence of equilibration seen from the $A = 3$ IYR probe (Fig. 5) than the isoscaling probe (Fig. 4) suggests that indeed the $A = 3$ IYR probe is less sensitive to secondary decay.

Integrating over impact parameters gives an average Γ_{eq} for each reaction. For the ^{64}Zn, ^{64}Ni + ^{64}Zn, ^{64}Ni reactions we calculate a Γ_{eq} of 0.77 ± 0.04. For the ^{64,70}Zn + ^{64,70}Zn reactions we calculate a Γ_{eq} of 0.72 ± 0.04. These values are reported in Table I.

C. Reconstructed quasiprojectile asymmetry

The isoscaling α parameter and the isobaric yield ratio are indirect metrics of the source asymmetry. The $\frac{N-Z}{A}$ of the QP can be measured directly using isotopically identified particles in the NIMROD 4π detector to reconstruct the QP. In this work the NIMROD array also measured the neutron multiplicity. This gives us a direct measure of the source asymmetry via reconstruction of the QP.

Keksis *et al.* [62,80] improved a technique, initially developed by Rowland [81], to reconstruct the hot postinteraction QP from its breakup into various charged fragments. By making appropriate cuts on the detected charged particles to remove contamination from pre-equilibrium emission and neck region emission, the remaining particles could be backtracked to reconstruct the hot QP immediately following reseparation of the QP-QT pair. This reconstruction gave a value of fractional equilibration (described subsequently) of 0.53, consistent with [21,62]. This marked the first attempt to experimentally determine the asymmetry of the source directly (rather than rely on a surrogate for the isospin asymmetry), and apply it to an equilibration study. Experiments conducted using the NIMROD array [23] determined that the quality of isoscaling fits could be greatly improved by selecting not only on reconstructed QPs, but also by including free neutron information. This allows a more detailed reconstruction of the QP, in particular its isospin asymmetry $\frac{N-Z}{A}$. In this work a well-defined hot QP was reconstructed by applying rigorous source cuts. We assumed that this reconstructed QP is the state immediately following the interaction and reseparation of the projectile and target. Note that the reconstructed total nucleon number cut (Sum$A$) selects QPs that are slightly more neutron-rich on average. Since the effect is similar for all the systems it does not affect the data shown in Fig. 6(b).

Figure 6(a) shows the reconstructed QP asymmetry Δ_{QP} as a function of the $v_{z,QP}$, while Fig. 6(b) shows the R_i when substituted with QP asymmetry Δ_{QP}. We do see evidence of isospin equilibration since the cross systems ^{64}Ni + ^{64}Zn and ^{64}Zn + ^{64}Ni lie between the symmetric systems. However, there is little to no change in Δ_{QP} between the two cross reactions and the data show no obvious convergence as a function of impact parameters, indicating that the degree of equilibration does not depend on the impact parameter.

This observation for Δ_{QP} is surprising considering that these reactions showed a dependence of the degree of equilibration on the impact parameter when analyzed using isoscaling (Fig. 4) and isobaric yield ratios (Fig. 5). One explanation for this observation is the correlation between the velocity damping and neutron multiplicity. Violent collisions produce slower PLFs and more free neutrons, protons, and low mass fragments. Thus the uncertainty in the neutron multiplicity measurement might wash out the convergence of the cross systems toward each other. Another possible explanation is the effect of secondary decay on the isotope yields. The $A = 64$ QP Δ_{QP} data also show a strong neutron-rich enhancement in the QP asymmetry for the cross reactions relative to the center of the two symmetric reactions.

Integrating over the impact parameter gives a Γ_{eq} of 0.85 ± 0.05 for the ^{64}Zn, ^{64}Ni + ^{64}Zn, ^{64}Ni reactions. For the ^{64,70}Zn + ^{64,70}Zn reactions we calculate a Γ_{eq} of 0.96 ± 0.05.

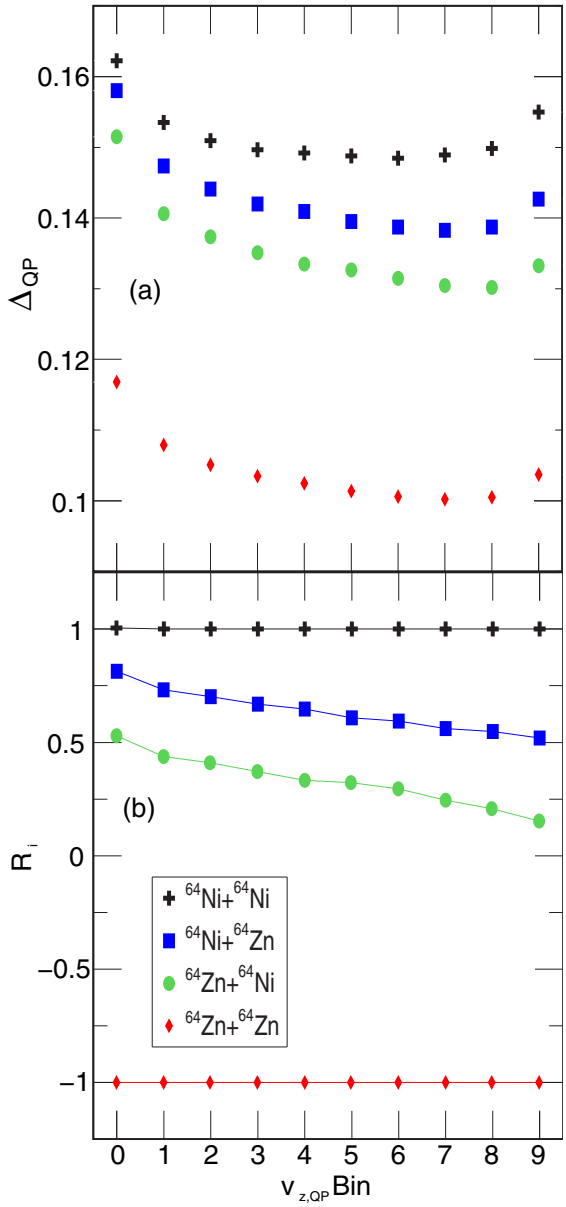

FIG. 6. (a) Quasiprojectile asymmetry Δ_{QP} as a function of $v_{z,QP}$ bin. (b) Isospin transport ratio R_i for the QP Δ_{QP} as a function of $v_{z,QP}$ bin. Data for the $A = 64$ set of reaction systems are shown: ^{64}Ni + ^{64}Ni, ^{64}Ni + ^{64}Zn, ^{64}Zn + ^{64}Ni, and ^{64}Zn + ^{64}Zn.

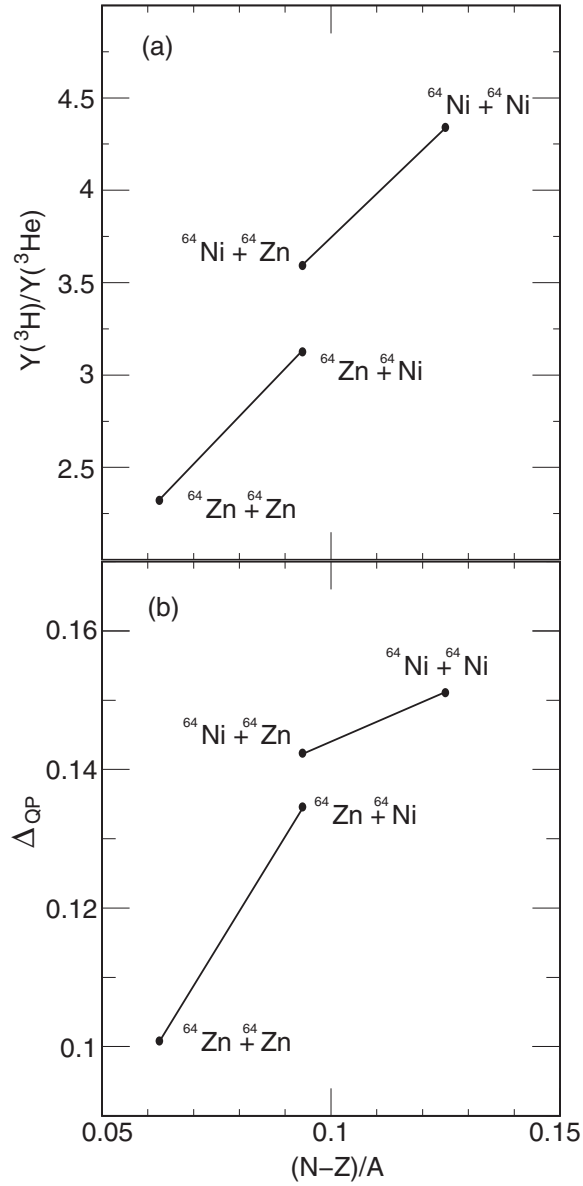

FIG. 7. Analysis from this work reproducing the right side of Fig. 2 for the $A = 64$ (^{64}Zn, ^{64}Ni + ^{64}Zn, ^{64}Ni) reaction systems using (a) the $A = 3$ isobaric yield ratio and (b) Δ_{QP} observables. (a) Ratio of yields $Y(^3H)/Y(^3He)$ for the $A = 64$ set of reactions as a function of the composite system isospin asymmetry. (b) Reconstructed Δ_{QP} for the same reaction set as a function of the composite system isospin asymmetry.

D. Integrating over $v_{z,QP}$

The isobaric yield ratio $Y(^3H)/Y(^3He)$ and the reconstructed Δ_{QP} are plotted as functions of composite system asymmetry in Fig. 7, similar to Figs. 2(b) and 2(d). Solid black lines connect systems with the same projectile. $Y(^3H)/Y(^3He)$ and Δ_{QP} of the cross reactions differ from those of the symmetric reactions. Similar to the results from the isoscaling metric α this difference can be interpreted as a degree of mixing between the projectile and target, but not complete mixing. For both metrics the cross reactions are not centered around the midpoint between the two symmetric systems.

We recall that the R_i used in [21] assumes that a fully N-Z equilibrated cross system will be halfway between that of the two symmetric systems from the same reaction set. This assumption is limiting because the equilibrium value of an isospin observable is not necessarily halfway between the values for the symmetric systems. Figure 7 highlights the importance of using a technique that compares the separation between cross systems to the separation between symmetric systems to extract a value of fractional equilibration Γ_{eq}. Thus any differential loss outside of the QP-QT pair, through pre-equilibrium particle emission or neck formation, does not

affect the calculation of how much equilibration has taken place. Analysis predicated on the assumption of convergence to a midway point would under represent the degree of equilibration in the ^{64}Ni + ^{64}Zn system, and over represent the degree of equilibration in the ^{64}Zn + ^{64}Ni system [Fig. 7(b)].

IV. SUMMARY AND CONCLUSIONS

We have presented an analysis of neutron-proton equilibration in heavy-ion reactions around the Fermi energy using three independent probes of the equilibration: (1) the isoscaling parameter α, (2) the $A = 3$ isobaric yield ratio $Y(^3\mathrm{H})/Y(^3\mathrm{He})$, and (3) the neutron-proton composition of the Δ_{QP} as reconstructed with a 4π detector. The values of Γ_{eq} presented in this work are consistent among the three different probes employed. Incomplete *N*-*Z* equilibration is observed. A clear dependence of the degree of equilibration on the collision violence (impact parameter) is seen. Equilibration is not necessarily seen when an observable reaches a value midway between two reference points; rather, equilibration is seen when the same observable measured in two reaction systems, which are spatial reflections of each other, reaches a common value. Given this observation, an appropriate method for calculating the degree of equilibration is proposed. The degree of equilibration is calculated for each method, and reasonable agreement is observed. The method is applied to data taken at higher beam energy; less equilibration is observed as would be expected from a reduced interaction time [47,48].

The equilibration chronometry technique presented in Refs. [82,83] found the rate of neutron-proton equilibration to follow first-order kinetics with a rate constant of 3 inverse zeptoseconds (10^{-21} seconds), across a range of systems at one energy. The technique presented in this work can probe equilibration at various beam energies. A complementary approach employing both can explore the sensitivity of model predictions to the fundamental interaction, in particular the asymmetry energy, in order to constrain the equation of state.

ACKNOWLEDGMENTS

This material is based upon work supported by the US Department of Energy, Office of Science, Office of Nuclear Physics under Award No. DE—FG02-93ER40773, and the Welch Foundation under Award No. A-1266. We thank the staff of the TAMU Cyclotron Institute for their exemplary standard of technical support and particle beams.

[1] V. Baran, M. Colonna, V. Greco, and M. Ditoro, Phys. Rep. **410**, 335 (2005).
[2] A. W. Steiner and B.-A. Li, Phys. Rev. C **72**, 041601(R) (2005).
[3] J. M. Lattimer and M. Prakash, Science **304**, 536 (2004).
[4] D. V. Shetty, S. J. Yennello, and G. A. Souliotis, Phys. Rev. C **76**, 024606 (2007).
[5] T. Klähn, D. Blaschke, S. Typel, E. N. E. van Dalen, A. Faessler, C. Fuchs, T. Gaitanos, H. Grigorian, A. Ho, E. E. Kolomeitsev, M. C. Miller, G. Röpke, J. Trümper, D. N. Voskresensky, F. Weber, and H. H. Wolter, Phys. Rev. C **74**, 035802 (2006).
[6] M. B. Tsang, Y. Zhang, P. Danielewicz, M. Famiano, Z. Li, W. G. Lynch, and A. W. Steiner, Phys. Rev. Lett. **102**, 122701 (2009).
[7] G. Giuliani, H. Zheng, and A. Bonasera, Prog. Part. Nucl. Phys. **76**, 116 (2014).
[8] M. A. Famiano, T. Liu, W. G. Lynch, M. Mocko, A. M. Rogers, M. B. Tsang, M. S. Wallace, R. J. Charity, S. Komarov, D. G. Sarantites, L. G. Sobotka, and G. Verde, Phys. Rev. Lett. **97**, 052701 (2006).
[9] H.-l. Liu, G.-C. Yong, and D.-H. Wen, Phys. Rev. C **91**, 044609 (2015).
[10] T. X. Liu, W. G. Lynch, M. B. Tsang, X. D. Liu, R. Shomin, W. P. Tan, G. Verde, A. Wagner, H. F. Xi, H. S. Xu, B. Davin, Y. Larochelle, R. T. de Souza, R. J. Charity, and L. G. Sobotka, Phys. Rev. C **76**, 034603 (2007).
[11] C. W. Ma, J. Yu, X. M. Bai, Y. L. Zhang, H. L. Wei, and S. S. Wang, Phys. Rev. C **89**, 057602 (2014).
[12] S. Mallik and G. Chaudhuri, Phys. Lett. B **727**, 282 (2013).
[13] L. Ou, M. Liu, and Z. Li, Phys. Rev. C **89**, 011001 (2014).
[14] G. Chaudhuri and S. Mallik, Nucl. Phys. A **849**, 190 (2011).
[15] S. Galanopoulos, G. Souliotis, A. Keksis, M. Veselsky, Z. Kohley, L. May, D. Shetty, S. Soisson, B. Stein, S. Wuenschel, and S. Yennello, Nucl. Phys. A **837**, 145 (2010).
[16] S. Kowalski, J. B. Natowitz, S. Shlomo, R. Wada, K. Hagel, J. Wang, T. Materna, Z. Chen, Y. G. Ma, L. Qin, A. S. Botvina, D. Fabris, M. Lunardon, S. Moretto, G. Nebbia, S. Pesente, V. Rizzi, G. Viesti, M. Cinausero, G. Prete, T. Keutgen, Y. El Masri, Z. Majka, and A. Ono, Phys. Rev. C **75**, 014601 (2007).
[17] A. Ono, P. Danielewicz, W. A. Friedman, W. G. Lynch, and M. B. Tsang, Phys. Rev. C **68**, 051601(R) (2003).
[18] G. A. Souliotis, D. V. Shetty, A. Keksis, E. Bell, M. Jandel, M. Veselsky, and S. J. Yennello, Phys. Rev. C **73**, 024606 (2006).
[19] G. A. Souliotis, P. N. Fountas, M. Veselsky, S. Galanopoulos, Z. Kohley, A. McIntosh, S. J. Yennello, and A. Bonasera, Phys. Rev. C **90**, 064612 (2014).
[20] M. B. Tsang, C. K. Gelbke, X. D. Liu, W. G. Lynch, W. P. Tan, G. Verde, H. S. Xu, W. A. Friedman, R. Donangelo, S. R. Souza, C. B. Das, S. Das Gupta, and D. Zhabinsky, Phys. Rev. C **64**, 054615 (2001).
[21] M. B. Tsang, T. X. Liu, L. Shi, P. Danielewicz, C. K. Gelbke, X. D. Liu, W. G. Lynch, W. P. Tan, G. Verde, A. Wagner, H. S. Xu, W. A. Friedman, L. Beaulieu, B. Davin, R. T. de Souza, Y. Larochelle, T. Lefort, R. Yanez, V. E. Viola, R. J. Charity, and L. G. Sobotka, Phys. Rev. Lett. **92**, 062701 (2004).
[22] M. Veselsky, G. A. Souliotis, and M. Jandel, Phys. Rev. C **69**, 044607 (2004).
[23] S. Wuenschel, R. Dienhoffer, G. A. Souliotis, S. Galanopoulos, Z. Kohley, K. Hagel, D. V. Shetty, K. Huseman, L. W. May, S. N. Soisson, B. C. Stein, A. L. Caraley, and S. J. Yennello, Phys. Rev. C **79**, 061602(R) (2009).
[24] F. Yao, F. De-Qing, M. Yu-Gang, C. Xiang-Zhou, T. Wen-Dong, W. Hong-Wei, and G. Wei, Chin. Phys. Lett. **26**, 082503 (2009).
[25] P. Zhou, W. D. Tian, Y. G. Ma, X. Z. Cai, D. Q. Fang, and H. W. Wang, Phys. Rev. C **84**, 037605 (2011).
[26] V. Baran, M. Colonna, and M. Di Toro, Nucl. Phys. A **730**, 329 (2004).

[27] L.-W. Chen, C. M. Ko, and B.-A. Li, Phys. Rev. Lett. **94**, 032701 (2005).

[28] E. Galichet, M. F. Rivet, B. Borderie, M. Colonna, R. Bougault, A. Chbihi, R. Dayras, D. Durand, J. D. Frankland, D. C. R. Guinet, P. Lautesse, N. Le Neindre, O. Lopez, L. Manduci, M. Pârlog, E. Rosato, B. Tamain, E. Vient, C. Volant, and J. P. Wieleczko (INDRA Collaboration), Phys. Rev. C **79**, 064614 (2009).

[29] Z. Y. Sun, M. B. Tsang, W. G. Lynch, G. Verde, F. Amorini, L. Andronenko, M. Andronenko, G. Cardella, M. Chatterje, P. Danielewicz, E. De Filippo, P. Dinh, E. Galichet, E. Geraci, H. Hua, E. La Guidara, G. Lanzalone, H. Liu, F. Lu, S. Lukyanov, C. Maiolino, A. Pagano, S. Piantelli, M. Papa, S. Pirrone, G. Politi, F. Porto, F. Rizzo, P. Russotto, D. Santonocito, and Y. X. Zhang, Phys. Rev. C **82**, 051603 (2010).

[30] H. S. Xu, M. B. Tsang, T. X. Liu, X. D. Liu, W. G. Lynch, W. P. Tan, A. Vander Molen, G. Verde, A. Wagner, H. F. Xi, C. K. Gelbke, L. Beaulieu, B. Davin, Y. Larochelle, T. Lefort, R. T. de Souza, R. Yanez, V. E. Viola, R. J. Charity, and L. G. Sobotka, Phys. Rev. Lett. **85**, 716 (2000).

[31] Z. W. Kohley, Ph.D. thesis, Texas A&M University, 2010.

[32] Z. Kohley, L. W. May, S. Wuenschel, A. Bonasera, K. Hagel, R. Tripathi, R. Wada, G. A. Souliotis, D. V. Shetty, S. Galanopoulos, M. Mehlman, W. B. Smith, S. N. Soisson, B. C. Stein, and S. J. Yennello, Phys. Rev. C **82**, 064601 (2010).

[33] Z. Kohley, L. W. May, S. Wuenschel, M. Colonna, M. Di Toro, M. Zielinska-Pfabe, K. Hagel, R. Tripathi, A. Bonasera, G. A. Souliotis, D. V. Shetty, S. Galanopoulos, M. Mehlman, W. B. Smith, S. N. Soisson, B. C. Stein, and S. J. Yennello, Phys. Rev. C **83**, 044601 (2011).

[34] X. Liu, W. Lin, R. Wada, M. Huang, Z. Chen, G. Q. Xiao, S. Zhang, R. Han, M. H. Zhao, P. Ren, Z. Jin, J. Liu, F. Shi, J. B. Natowitz, A. Bonasera, K. Hagel, H. Zheng, M. Barbui, and K. Schmidt, Phys. Rev. C **90**, 014604 (2014).

[35] P. Russotto, P. Wu, M. Zoric, M. Chartier, Y. Leifels, R. Lemmon, Q. Li, J. Łukasik, A. Pagano, P. Pawłowski, and W. Trautmann, Phys. Lett. B **697**, 471 (2011).

[36] P. Russotto, M. D. Cozma, A. Le Fèvre, Y. Leifels, R. Lemmon, Q. Li, J. Łukasik, and W. Trautmann, Eur. Phys. J. A **50**, 38 (2014).

[37] L. Scalone, M. Colonna, and M. Di Toro, Phys. Lett. B **461**, 9 (1999).

[38] E. De Filippo and A. Pagano, Eur. Phys. J. A **50**, 32 (2014).

[39] M. Di Toro, A. Olmi, and R. Roy, Eur. Phys. J. A **30**, 65 (2006).

[40] S. Hudan, R. Alfaro, L. Beaulieu, B. Davin, Y. Larochelle, T. Lefort, V. E. Viola, H. Xu, R. Yanez, R. T. de Souza, R. J. Charity, L. G. Sobotka, T. X. Liu, X. D. Liu, W. G. Lynch, R. Shomin, W. P. Tan, M. B. Tsang, A. Vander Molen, A. Wagner, and H. F. Xi, Phys. Rev. C **70**, 031601 (2004).

[41] J. Łukasik, J. Benlliure, V. Métivier, E. Plagnol, B. Tamain, M. Assenard, G. Auger, C. O. Bacri, E. Bisquer, B. Borderie, R. Bougault, R. Brou, P. Buchet, J. L. Charvet, A. Chbihi, J. Colin, D. Cussol, R. Dayras, A. Demeyer, D. Doré, D. Durand, E. Gerlic, S. Germain, D. Gourio, D. Guinet, P. Lautesse, J. L. Laville, J. F. Lecolley, A. Le Fèvre, T. Lefort, R. Legrain, O. Lopez, M. Louvel, N. Marie, L. Nalpas, M. Parlog, J. Péter, O. Politi, A. Rahmani, T. Reposeur, M. F. Rivet, E. Rosato, F. Saint-Laurent, M. Squalli, J. C. Steckmeyer, M. Stern, L. Tassan-Got, E. Vient, C. Volant, J. P. Wieleczko, M. Colonna, F. Haddad, P. Eudes, T. Sami, and F. Sebille, Phys. Rev. C **55**, 1906 (1997).

[42] A. B. McIntosh, S. Hudan, J. Black, D. Mercier, C. J. Metelko, R. Yanez, R. T. de Souza, A. Chbihi, M. Famiano, M. O. Frégeau, J. Gauthier, J. Moisan, R. Roy, S. Bianchin, C. Schwarz, and W. Trautmann, Phys. Rev. C **81**, 034603 (2010).

[43] C. P. Montoya, W. G. Lynch, D. R. Bowman, G. F. Peaslee, N. Carlin, R. T. de Souza, C. K. Gelbke, W. G. Gong, Y. D. Kim, M. A. Lisa, L. Phair, M. B. Tsang, J. B. Webster, C. Williams, N. Colonna, K. Hanold, M. A. McMahan, G. J. Wozniak, and L. G. Moretto, Phys. Rev. Lett. **73**, 3070 (1994).

[44] J. Tõke, B. Lott, S. Baldwin, B. Quednau, W. Schröder, L. Sobotka, J. Barreto, R. Charity, L. Gallamore, D. Sarantites, D. Stracener, and R. De Souza, Nucl. Phys. A **583**, 519 (1995).

[45] S. Yennello, B. Young, J. Yee, J. Winger, J. Winfield, G. Westfall, A. Molen, B. Sherrill, J. Shea, E. Norbeck, D. Morrissey, T. Li, E. Gualtieri, D. Craig, W. Benenson, and D. Bazin, Phys. Lett. B **321**, 15 (1994).

[46] B.-A. Li and S. J. Yennello, Phys. Rev. C **52**, R1746 (1995).

[47] H. Johnston, T. White, J. Winger, D. Rowland, B. Hurst, F. Gimeno-Nogues, D. O'Kelly, and S. Yennello, Phys. Lett. B **371**, 186 (1996).

[48] H. Johnston, T. White, B. A. Li, E. Ramakrishnan, J. Winger, D. J. Rowland, B. Hurst, F. Gimeno-Nogues, D. O'Kelly, Y.-W. Lui, and S. J. Yennello, Phys. Rev. C **56**, 1972 (1997).

[49] F. Rami, Y. Leifels, de Schauenburg B, A. Gobbi, B. Hong, J. Alard, A. Andronic, R. Averbeck, V. Barret, Z. Basrak, N. Bastid, I. Belyaev, A. Bendarag, G. Berek, R. Caplar, N. Cindro, P. Crochet, A. Devismes, P. Dupieux, M. Dzelalija, M. Eskef, C. Finck, Z. Fodor, H. Folger, L. Fraysse, and A. Genoux-Lubain, Phys. Rev. Lett. **84**, 1120 (2000).

[50] G. Ademard, B. Borderie, A. Chbihi, O. Lopez, P. Napolitani, M. F. Rivet, M. Boisjoli, E. Bonnet, R. Bougault, J. D. Frankland, E. Galichet, D. Guinet, M. Kabtoul, G. Lehaut, P. Lautesse, M. L. Commara, N. L. Neindre, P. Marini, P. Pawlowski, E. Rosato, R. Roy, E. Spadaccini, E. Vient, M. Vigilante, J. P. Wieleczko, D. Gruyer, M. La Commara, N. Le Neindre, M. Pârlog, P. Pawłowski, and G. Spadaccini, Eur. Phys. J. A **50**, 33 (2014).

[51] M. Colonna, V. Baran, and M. Di Toro, Eur. Phys. J. A **50**, 30 (2014).

[52] Z. Kohley and S. J. Yennello, Eur. Phys. J. A **50**, 31 (2014).

[53] V. Baran, M. Colonna, M. Di. Toro, M. Zielinska-Pfabé, and H. H. Wolter, Phys. Rev. C **72**, 064620 (2005).

[54] M. Colonna and M. B. Tsang, Eur. Phys. J. A **30**, 165 (2006).

[55] L.-W. Chen, C. M. Ko, B.-A. Li, C. Xu, and J. Xu, Eur. Phys. J. A **50**, 29 (2014).

[56] R. Planeta, S. H. Zhou, K. Kwiatkowski, W. G. Wilson, V. E. Viola, H. Breuer, D. Benton, F. Khazaie, R. J. McDonald, A. C. Mignerey, A. Weston-Dawkes, R. T. de Souza, J. R. Huizenga, and W. U. Schröder, Phys. Rev. C **38**, 195 (1988).

[57] W. U. Schröder and J. R. Huizenga, Annu. Rev. Nucl. Sci. **27**, 465 (1977).

[58] W. U. Schröder, J. R. Birkelund, J. R. Huizenga, K. L. Wolf, and V. E. Viola, Phys. Rev. C **16**, 623 (1977).

[59] M. B. Tsang, W. A. Friedman, C. K. Gelbke, W. G. Lynch, G. Verde, and H. S. Xu, Phys. Rev. Lett. **86**, 5023 (2001).

[60] S. Barlini, S. Piantelli, G. Casini, P. R. Maurenzig, A. Olmi, M. Bini, S. Carboni, G. Pasquali, G. Poggi, a. a. Stefanini, R. Bougault, E. Bonnet, B. Borderie, A. Chbihi, J. D. Frankland, D. Gruyer, O. Lopez, N. Le Neindre, M. Pârlog, M. F. Rivet, E. Vient, E. Rosato, G. Spadaccini, M. Vigilante, M. Bruno, T. Marchi, L. Morelli, M. Cinausero, M. Degerlier, F. Gramegna,

T. Kozik, T. Twaróg, R. Alba, C. Maiolino, and D. Santonocito (FAZIA Collaboration), Phys. Rev. C **87**, 054607 (2013).
[61] S. Hudan and R. T. DeSouza, Eur. Phys. J. A **50**, 36 (2014).
[62] A. L. Keksis, L. W. May, G. A. Souliotis, M. Veselsky, S. Galanopoulos, Z. Kohley, D. V. Shetty, S. N. Soisson, B. C. Stein, R. Tripathi, S. Wuenschel, S. J. Yennello, and B. A. Li, Phys. Rev. C **81**, 054602 (2010).
[63] E. Bell, Ph.D. thesis, Texas A&M University, 2005.
[64] R. Ghetti and J. Helgesson, Nucl. Phys. A **752**, 480 (2005).
[65] E. Galichet, M. Colonna, B. Borderie, and M. F. Rivet, Phys. Rev. C **79**, 064615 (2009).
[66] B. Yilmaz, S. Ayik, D. Lacroix, and O. Yilmaz, Phys. Rev. C **90**, 024613 (2014).
[67] J. M. Lattimer and Y. Lim, Astrophys. J. **771**, 51 (2013).
[68] S. Wuenschel, K. Hagel, R. Wada, J. Natowitz, S. Yennello, Z. Kohley, C. Bottosso, L. May, W. Smith, D. Shetty, B. Stein, S. Soisson, and G. Prete, Nucl. Instrum. Methods Phys. Res., Sect. A **604**, 578 (2009).
[69] L. W. May, Ph.D. thesis, Texas A&M University, 2015.
[70] S. K. Wuenschel, Ph.D. thesis, Texas A&M University, 2009.
[71] A. McIntosh, A. Bonasera, P. Cammarata, K. Hagel, L. Heilborn, Z. Kohley, J. Mabiala, L. May, P. Marini, A. Raphelt, G. Souliotis, S. Wuenschel, A. Zarrella, and S. Yennello, Phys. Lett. B **719**, 337 (2013).
[72] S. Wuenschel, A. Bonasera, L. May, G. Souliotis, R. Tripathi, S. Galanopoulos, Z. Kohley, K. Hagel, D. Shetty, K. Huseman, S. Soisson, B. Stein, and S. Yennello, Nucl. Phys. A **843**, 1 (2010).
[73] P. Marini, A. Bonasera, A. McIntosh, R. Tripathi, S. Galanopoulos, K. Hagel, L. Heilborn, Z. Kohley, L. W. May, M. Mehlman, S. N. Soisson, G. A. Souliotis, D. V. Shetty, W. B. Smith, B. C. Stein, S. Wuenschel, and S. J. Yennello, Phys. Rev. C **85**, 034617 (2012).
[74] J. Steckmeyer, E. Genouin-Duhamel, E. Vient, J. Colin, D. Durand, G. Auger, C. Bacri, N. Bellaize, B. Borderie, R. Bougault, B. Bouriquet, R. Brou, P. Buchet, J. Charvet, A. Chbihi, D. Cussol, R. Dayras, N. De Cesare, A. Demeyer, D. Doré, J. Frankland, E. Galichet, E. Gerlic, D. Guinet, S. Hudan, P. Lautesse, F. Lavaud, J. Laville, J. Lecolley, C. Leduc, R. Legrain, N. Le Neindre, O. Lopez, M. Louvel, A. Maskay, L. Nalpas, J. Normand, M. Pârlog, P. Pawłowski, E. Plagnol, M. Rivet, E. Rosato, F. Saint-Laurent, G. Tăbăcaru, B. Tamain, L. Tassan-Got, O. Tirel, K. Turzo, M. Vigilante, C. Volant, and J. Wieleczko, Nucl. Phys. A **686**, 537 (2001).
[75] D. J. Hinde, D. Hilscher, and H. Rossner, Nucl. Phys. A **502**, 497 (1989).
[76] P. Marini, A. Zarrella, A. Bonasera, G. Bonasera, P. Cammarata, L. Heilborn, Z. Kohley, J. Mabiala, L. May, A. McIntosh, A. Raphelt, G. Souliotis, and S. Yennello, Nucl. Instrum. Methods Phys. Res., Sect. A **707**, 80 (2013).
[77] A. B. McIntosh, A. Bonasera, Z. Kohley, P. J. Cammarata, K. Hagel, L. Heilborn, J. Mabiala, L. W. May, P. Marini, A. Raphelt, G. A. Souliotis, S. Wuenschel, A. Zarrella, and S. J. Yennello, Phys. Rev. C **87**, 034617 (2013).
[78] M. Papa, T. Maruyama, and A. Bonasera, Phys. Rev. C **64**, 024612 (2001).
[79] M. Papa, G. Giuliani, and A. Bonasera, J. Comput. Phys. **208**, 403 (2005).
[80] A. L. Keksis, Ph.D. thesis, Texas A&M University, 2007.
[81] D. J. Rowland, Ph.D. thesis, Texas A&M University, 2000.
[82] A. Jedele, A. B. McIntosh, K. Hagel, M. Huang, L. Heilborn, Z. Kohley, L. W. May, E. McCleskey, M. Youngs, A. Zarrella, and S. J. Yennello, Phys. Rev. Lett. **118**, 062501 (2017).
[83] A. Rodriguez Manso, A. B. McIntosh, A. Jedele, K. Hagel, L. Heilborn, Z. Kohley, L. W. May, A. Zarrella, and S. J. Yennello, Phys. Rev. C **95**, 044604 (2017).